

## Band dispersions of the $\pi$ -bonded-chain reconstruction of Si(111) $3\times 1$ -Li: A critical evaluation of theory and experiment

H. H. Weitering and X. Shi

*Department of Physics and Astronomy, The University of Tennessee, Knoxville, Tennessee 37996  
and Solid State Division, Oak Ridge National Laboratory, Oak Ridge, Tennessee 37831*

S. C. Erwin

*Complex Systems Theory Branch, Code 6691, Naval Research Laboratory, Washington, D.C. 20375  
(Received 23 May 1996)*

The surface-state band-structure of the three-domain Si(111) $3\times 1$ -Li reconstruction has been determined using angle-resolved photoemission. Experimental band dispersions are compared to theoretical calculations for the extended Pandey model and the Seiwatz model. Even though the extended Pandey model is favored on the basis of scanning tunneling microscopy and total-energy considerations, the calculated surface states are inconsistent with experiment. The calculated states for the Seiwatz model are consistent with the experimental dispersion along the main symmetry direction ( $\bar{\Gamma}-\bar{A}$ ) but serious discrepancies exist in other parts of the Brillouin zone. The disparity between the density-functional-theory calculations and experiment indicate that exchange and correlation in  $\pi$ -bonded Si chains may need to be analyzed beyond the mean-field band-structure approach. [S0163-1829(96)03039-1]

### I. INTRODUCTION

The complexity of semiconductor surface reconstructions poses a tremendous challenge to the surface scientist. It took 26 years of combined efforts to solve the structure of the Si(111) $7\times 7$  surface.<sup>1,2</sup> Other reconstructions such as Si(111) $2\times 1$ ,<sup>3-5</sup> Si(111)( $\sqrt{3}\times\sqrt{3}$ ) $R30^\circ$ -Ag,<sup>6,7</sup> and Si(111) $5\times 2$ -Au (Ref. 8) were solved after many years of experimental and theoretical research. One of the main difficulties in establishing a "final" model is the need to reconcile the seemingly conflicting results from numerous experimental and theoretical studies. Generally speaking, surface x-ray diffraction is the most straightforward technique for the determination of the surface structure. Nonetheless, the "best fit" to the diffraction data still needs to be consistent with results from other measurements. For example, diffraction studies have led to conflicting structural models for the Si(111)( $\sqrt{3}\times\sqrt{3}$ ) $R30^\circ$ -Ag reconstruction.<sup>9,10</sup> The precise structural model was pinned down later when density-functional-theory calculations identified the honeycomb-chained-trimer model as the lowest total-energy configuration<sup>6</sup> and nicely reproduced published scanning tunneling microscopy (STM) images<sup>11</sup> and surface-state dispersions in angle-resolved photoemission.<sup>7,12</sup> Such a comparison between theory, STM, and angle-resolved photoemission data is also of paramount importance even if the interface structure has been firmly established by other means because it reveals how accurately state-of-the-art electronic structure calculations can reproduce the ground-state properties of the interface.

One puzzle that remains to be solved is the alkali-induced Si(111) $3\times 1$  reconstruction. This reconstruction has attracted considerable attention recently after it was found that this surface exhibited unusual chemical<sup>13</sup> and electronic properties.<sup>14</sup> Filled-state STM images of Si(111) $3\times 1$ -Na revealed the presence of zigzag rows of adatoms parallel to the

$[\bar{1}\bar{1}0]$  direction which are separated by dark channels. Several models have been proposed to explain these images.<sup>14-21</sup> However, with the determination of the absolute metal coverage ( $\frac{1}{3}$  ML),<sup>16</sup> the number of realistic candidates has been reduced to two, namely, the Seiwatz model<sup>16,17</sup> and the extended Pandey model<sup>20</sup> (Fig. 1).

The Seiwatz model [Fig. 1(a)] was first proposed by Weitering and co-workers<sup>16</sup> and later independently by Sakamoto and co-workers.<sup>17</sup> In this model, fivefold Si rings form quasi-one-dimensional  $\pi$ -bonded Si chains along  $[110]$ , separated by channels which can accommodate up to  $\frac{1}{3}$  ML of metal atoms. To account for the asymmetry in the STM

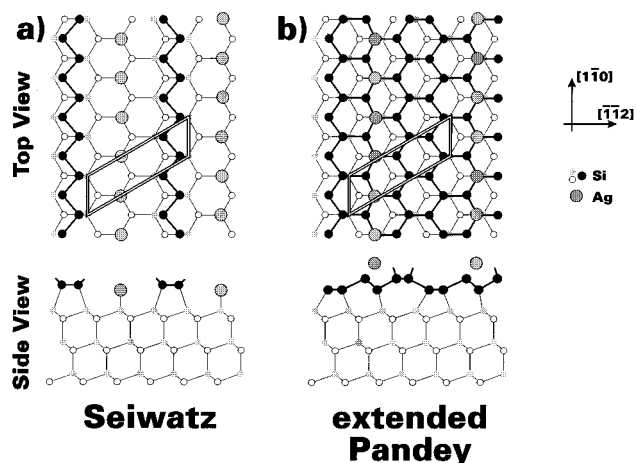


FIG. 1. Idealized geometries (unrelaxed and nonbuckled) of the Seiwatz model (a) and the extended Pandey model (b) for the metal-induced Si(111) $3\times 1$  reconstruction (Refs. 16 and 20). Total-energy calculations by Erwin suggest that the fivefold Si rings of the Seiwatz model and sevenfold rings of the extended Pandey model undergo a Jahn-Teller distortion, resulting in a buckling of the  $\pi$ -bonded Si chains.

image of Si(111)3×1-Li,<sup>15</sup> Weitering *et al.* suggested that the  $\pi$ -bonded chains exhibit a Peierls-like instability, resulting in a modulation of the Si-Si bond length along the chains.<sup>16</sup> This situation would resemble the dimerization in conjugated polymers such as polyacetylene.<sup>22</sup> The Seiwatz model also appeared to be the best fit to the x-ray-scattering data from the Si(111)3×1-Ca interface although the issue of dimerization was left open.<sup>23</sup>

The extended Pandey model [Fig. 1(b)] was introduced independently by Erwin<sup>20</sup> and by Okuda *et al.*,<sup>18</sup> and was proposed as the correct structural model on the basis of (i) first-principles total-energy calculations for Li, Na, K, and Rb adsorbates, and (ii) the close correspondence between theoretical and experimental STM images.<sup>20</sup> The total-energy results slightly favored the Pandey model relative to the Seiwatz model (by  $\sim 0.1$  eV/cell) for K and Rb but the difference was negligible ( $\sim 0.01$  eV/cell) for Li and Na. According to the calculations, the  $\pi$ -bonded chains of the fully relaxed Pandey and Seiwatz structures are buckled, *not* dimerized. Alternatives such as adsorption on the bulk-truncated surfaces and substitutional models were found to be *significantly* higher in energy.

In this paper, we present angle-resolved photoemission data of the Si(111)3×1-Li surface and compare the results with density-functional-theory calculations of the surface-state dispersions for the Seiwatz model and extended Pandey model. In addition, we present Si  $2p$  and Li  $1s$  core-level photoemission data. The experimental surface-state dispersions agree in part with those calculated for the relaxed Seiwatz reconstruction but this agreement does not hold throughout the full surface Brillouin zone. Furthermore, the zigzag chains observed in STM are inconsistent with the relaxed Seiwatz reconstruction. The relaxed Pandey reconstruction predicts a  $\pi$ -bonded chain surface state that is strongly at odds with our photoemission data. However, previously published STM data are consistent with this model. We will discuss several scenarios that possibly account for these discrepancies.

## II. EXPERIMENTAL AND COMPUTATIONAL PROCEDURES

Angle-resolved photoemission experiments were carried out at beam line U12b of the National Synchrotron Light Source at Brookhaven National Laboratory. The incident light was dispersed by a toroidal grating monochromator. The total-energy resolution is 0.15 eV at a photon energy of 21.2 eV and 0.5 eV at a photon energy of 100 eV. The hemispherical analyzer has an acceptance angle of  $\pm 2^\circ$ . The Fermi level of the spectrometer was calibrated from the Fermi cutoff of a thick Li film, deposited near 77 K. Lightly doped *n*-type Si(111) wafers were cut into  $7 \times 20$  mm<sup>2</sup> samples, cleaned by the Shiraki method, and inserted into the vacuum chamber which had a base pressure of  $7 \times 10^{-11}$  mbar. The thin oxide layer was removed by direct resistive heating to 850 °C. After cooling to room temperature (RT), sharp (7×7) low-energy electron diffraction (LEED) patterns were consistently observed. The Si(111)3×1-Li reconstruction was prepared by exposing the clean Si(111)7×7 surface to a thoroughly degassed SAES Li getter source at a sample temperature of 580 °C. Special care was taken to thermally

quench the substrate as soon as the deposition was stopped. Otherwise, thermal desorption of the metal species would lead to a coexistence of (3×1) and (7×7) domains. After cooling to RT, high quality three-domain (3×1) (LEED) patterns were observed.

The theoretical dispersion curves for the Seiwatz and Pandey models were calculated from first principles, within the framework of the local-density approximation (LDA) to density-functional theory (DFT). The calculations were performed using the electronic-structure code of Teter, Payne, and Allan,<sup>24</sup> which solves the Kohn-Sham equations with a plane-wave basis using norm-conserving pseudopotentials. The two reconstructions were modeled by a slab-supercell geometry, and full structural relaxation was performed by following the Hellmann-Feynman forces until the root-mean-square forces were no more than 0.05 eV/Å; details of the computational procedure can be found in Ref. 20. For the dispersion curves, the slabs were passivated on one side with hydrogen in order to obtain a single set of surface states. From the full eigenvalue spectrum, surface states were identified by examining the electronic density associated with each separate band state. Only states with strong components on surface atoms were labeled as true surface states.

## III. RESULTS AND DISCUSSION

### A. The surface-state band structure

Figure 2 shows the valence-band photoemission spectra of a three-domain Si(111)3×1-Li surface for various emission angles. In Fig. 2(a) the light beam, polarization vector, and detector are all in the plane defined by the surface normal and the [110] direction (shaded plane in Fig. 3). Figure 2(a) thus represents the dispersion along the chain direction, i.e., [110]. Due to the threefold symmetry of the underlying substrate, the (3×1) surface is composed of three domains, making angles of 120° (Fig. 4). Accordingly, the spectra in Fig. 2(a) not only contain information about the surface-state dispersion along the  $[\bar{1}\bar{1}0]$  or  $\bar{\Gamma}\bar{A}$  direction but also along the  $\bar{\Gamma}\bar{D}$  direction. Likewise, the spectra in Fig. 2(b) contain information along  $\bar{\Gamma}\bar{C}$  and  $\bar{\Gamma}\bar{E}$ . These symmetry symbols for the (3×1) Brillouin zone follow the convention introduced by Sakamoto *et al.*<sup>17</sup> Unfortunately, it is impossible to deconvolute the contributions from the various domains. Nonetheless, the photoemission data reveal the presence of a prominent surface state or resonance which is marked by the solid line *S*. In Fig. 2(a), it emerges as a surface resonance near  $\Theta_e \approx 12.5^\circ$  and disperses downward along [110] to  $\bar{A}$  and  $\bar{K}$  ( $\Theta_e \approx 33^\circ$  at  $\bar{K}$ ) where it enters the gap region in the projected bulk band structure (Fig. 5). The measured band width is  $\approx 0.6$  eV. Note that the surface-state dispersion is *not* symmetric around the zone boundary at  $\bar{A}$  because  $\bar{A}$  coincides with the B point of the second (3×1) Brillouin zone [Fig. 4(a)]. We also measured the dispersion along the  $[\bar{1}\bar{1}2]$  or  $\bar{\Gamma}\bar{C}$  direction, i.e., normal to the chains, by moving the detector out of the horizontal plane. These spectra reveal a surface state which has a much smaller dispersion [ $\approx 0.1$  eV, Fig. 2(b)]. To accurately map the dispersion along  $\bar{\Gamma}\bar{C}$ , we determined the peak positions from the minima of the second derivatives. The experimental results are summarized in a dispersion plot in Fig. 5 (circles), using standard procedures.<sup>25</sup> The shaded areas in this plot represent the pro-

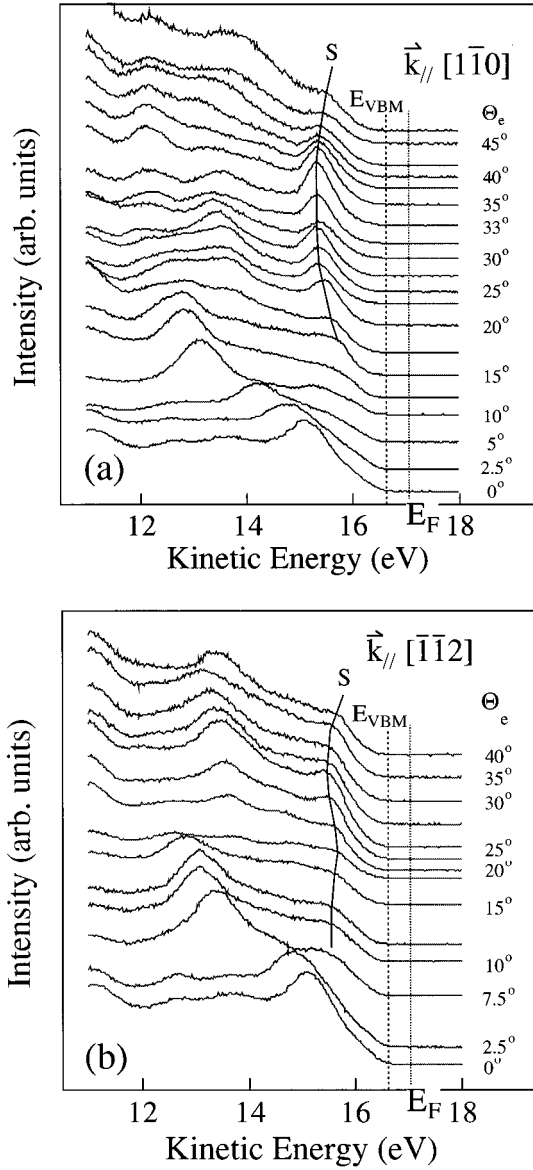


FIG. 2. Angle-resolved photoemission spectra of the three-domain Si(111) $3\times 1$ -Li surface along the (a)  $[1\bar{1}0]$  and (b)  $[\bar{1}\bar{1}2]$  direction for different emission angles  $\Theta_e$ . Surface states are “connected” by the solid lines  $S$  which are meant only as a guide to the eye. The polarization vector of the incident radiation is in the plane spanned by the  $[1\bar{1}0]$  vector and the surface normal (see also Fig. 3). The angle of incidence of  $\alpha_i$  is  $45^\circ$ . The photon energy is 21.2 eV. The valence-band maximum and Fermi energy are indicated by the vertical dashed and dotted lines, respectively.

jection of the bulk bands onto the (111) plane.<sup>26</sup> The energy scale is defined with respect to the valence-band maximum, as determined from Si  $2p$  core-level spectroscopy (Sec. III B). This makes it possible to compare the data directly with the dispersions from our first-principles calculations (solid lines in Fig. 5).

A few features in the spectra are worth mentioning. First of all, there is no emission intensity anywhere near  $E_F$  and hence the surface is semiconducting. Second, even though the surface consists of three domains, we measure a strong dispersion along the chain direction and a small dispersion perpendicular to the chains. This is precisely what one would

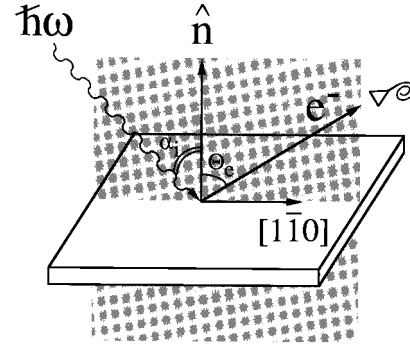


FIG. 3. Geometry of the angle-resolved photoemission experiment when probing the band dispersion along the chain direction [see Fig. 2(a)]. The polarization vector of the synchrotron light and the detector are both in the shaded plane which is defined by the surface normal  $\hat{n}$  and the  $[1\bar{1}0]$  direction. The angle of incidence  $\alpha_i$  is  $45^\circ$ .

expect for a single-domain surface. Furthermore, the experimental dispersion along  $\bar{\Gamma}\bar{C}$  seems to follow the symmetry of the  $3\times 1$  Brillouin-zone.

The solid lines in Fig. 5 are the *theoretical* dispersions of the filled states which possess a *genuine surface character*. The full theoretical band structure (including the bulk states) of the Seiwatz and extended Pandey models are shown in Figs. 6(a) and 6(b), respectively. In Fig. 5, the theoretical surface states of the extended Pandey model are offset by 0.55 eV in order to obtain a reasonable match with the experimental data points. No offset was needed for the Seiwatz

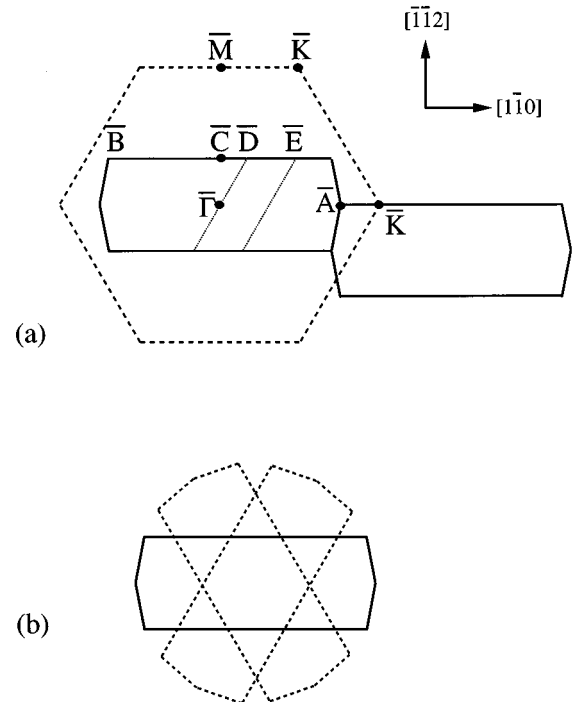


FIG. 4. (a) The surface Brillouin zones of the Si(111) $1\times 1$  (dashed) and Si(111) $3\times 1$ -Li reconstructions (solid lines). The dotted lines serve as a guide to the eye. (b) Three equivalent  $3\times 1$  Brillouin-zone-making angles of  $120^\circ$ . The symmetry symbols are identical to those introduced by Sakamoto *et al.* (Ref. 17).

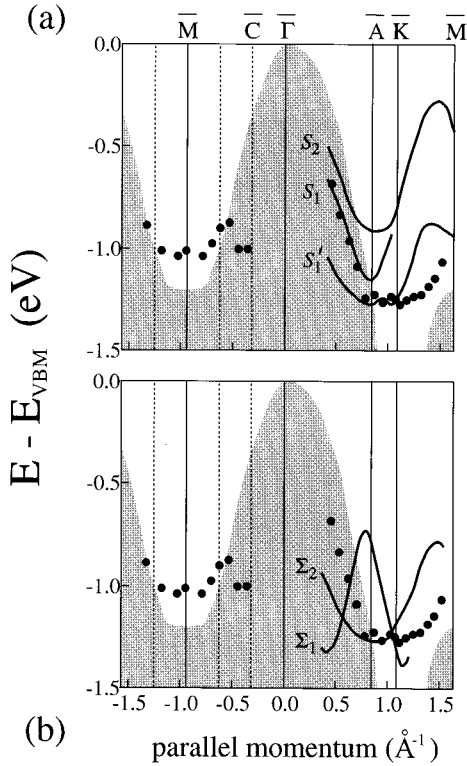


FIG. 5. Band dispersions of the Si(111) $3\times 1$ -Li surface. The filled circles are the experimental data. The solid lines are the calculated surface-state bands of the Seiwatz model (a) and extended Pandey model (b) with *buckled* geometries. In order to obtain a reasonable match between theory and experiment, the theoretical *surface-state bands* of the extended Pandey model were offset by 0.55 eV. No offset was needed for the Seiwatz states. The shaded areas represent the projected band structure as calculated by Ivanov, Mazur, and Pollmann (Ref. 26). The projected bulk bands in (a) and (b) are *not* vertically offset.

states. The most noticeable differences in the theoretical surface-state dispersions between the Seiwatz and Pandey models show up in the direction parallel to the  $\pi$ -bonded Si chains, i.e.,  $[1\bar{1}0]$ . Only subtle differences exist in the direction normal to the chain directions. In fact, the calculations did not reveal states with genuine surface character there.

According to theory, the extended Pandey reconstruction exhibits a filled surface state,  $\Sigma_1$ , which disperses *upward* along  $[1\bar{1}0]$  for wave vectors approaching the zone boundary at  $\bar{A}$ .<sup>20</sup> This is the surface state associated with the  $\pi$ -bonded Si chains and its dispersion is qualitatively similar to that of another  $\pi$ -bonded chain reconstruction, namely, Si(111) $2\times 1$ .<sup>3,5</sup> Another surface state,  $\Sigma_2$ , disperses *downward* along  $[1\bar{1}0]$  to  $\bar{A}$  and  $\bar{K}$ . This state is associated with the outermost Si atoms of the sixfold rings, i.e., the channel atoms.<sup>20</sup>  $\Sigma_2$  is roughly reproduced by experiment but the agreement is far from satisfactory. The most disturbing discrepancy, however, is the *absence of the upward dispersing  $\pi$ -bonded surface state in experiment*, i.e.,  $\Sigma_1$ .

The calculations for the Seiwatz reconstruction reveal three filled surface states (labeled  $S_1$ ,  $S_2$ , and  $S_1'$ ) which all disperse downward along the  $[1\bar{1}0]$  direction to  $\bar{A}$  and  $\bar{K}$ . The surface state  $S_2$  is clearly associated with the channel atoms throughout much of the Brillouin zone.  $S_1$  is the dou-

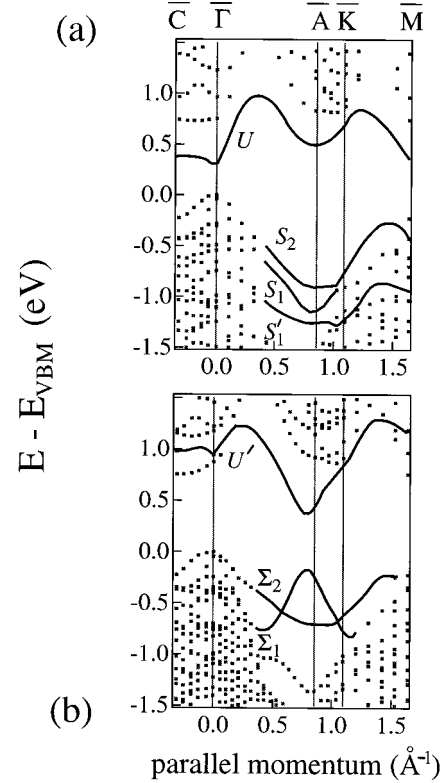


FIG. 6. Full band structure of the Seiwatz model (a) and extended Pandey model (b). The solid lines connect the electronic states which have a true surface character.  $U$  and  $U'$  are empty surface states.

bly occupied dangling-bond surface state of the “chain-up” atom of the  $\pi$ -bonded Si chains.  $S_1'$  has a large backbond component between  $\bar{\Gamma}$  and  $\bar{K}$  but at  $\bar{M}$  it has taken over the dangling-bond character of  $S_1$ .  $S_1$  is nicely reproduced by experiment between  $\bar{\Gamma}$  and  $\bar{A}$ . In between  $\bar{A}$  and  $\bar{K}$ , the data match  $S_1'$ . Assuming that the three surface states along  $\bar{\Gamma}\rightarrow\bar{A}\rightarrow\bar{K}$  cannot be properly resolved in experiment, there is a fairly good agreement between theory and experiment up to the  $\bar{K}$  point. However, serious discrepancies exist beyond the zone boundary when probing the “upper edge” of the second ( $3\times 1$ ) Brillouin zone (see Fig. 4). The channel-atom state  $S_2$  is clearly missing here (or too weak to be observed at large emission angles) whereas the calculated dispersion of  $S_1'$  is inconsistent with experiment. In this region,  $S_1'$  changes from a backbond state at  $\bar{K}$  to a dangling-bond surface state at  $\bar{M}$ ;  $S_1$  has lost its surface character in between  $\bar{A}$  and  $\bar{K}$ . Despite the discrepancy between theory and experiment beyond the  $\bar{K}$  point, we tentatively conclude that the angle-resolved photoemission data are in better agreement with the Seiwatz model. This will be discussed further in Sec. III C.

## B. The core levels

Si  $2p$  core levels were recorded with a photon energy of 120 eV (Fig. 7; see also Table I). This is close to the limits of our grating. The kinetic energy of the photoelectrons is thus  $\approx 15$  eV which means that the core-level spectra are not very surface sensitive. In order to enhance the surface sensitivity, we moved the detector away from the surface normal to

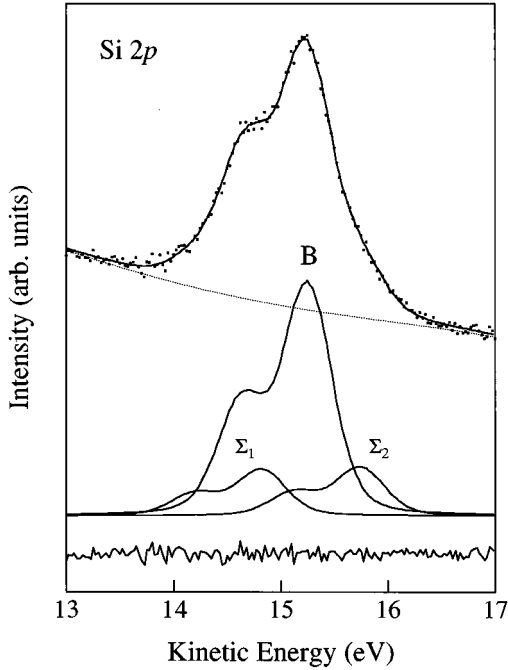


FIG. 7. Si  $2p$  core-level photoemission spectrum of Si(111) $3 \times 1$ -Li showing two surface core levels and one bulk component. The solid lines represent a nonlinear least squares fit to the experimental spectrum, using Lorentzian lineshapes with a FWHM of 150 meV, convoluted with a Gaussian (FWHM=0.43 eV). The background is a third-order polynomial function. Fitting parameters are given in Table I. The photon energy is 119.67 eV.

grazing exit angles. The best fit to the core-level spectrum includes one bulk component and two surface components of equal intensity, one on either side of the bulk peak. This deconvolution is very similar to that of the recently published high-resolution Si  $2p$  core-level spectra of Si(111) $3 \times 1$ -Na (Refs. 18, 27, and 28) and is also remarkably similar to that of Si(111) $2 \times 1$ .<sup>29</sup> Compared to the clean Si(111) $7 \times 7$  surface, the bulk component has shifted 0.20 eV toward lower binding energy. The Fermi level ( $E_F$ ) at the ( $7 \times 7$ ) surface is pinned at 0.63 eV above the valence-band maximum (VBM).<sup>30</sup> We thus infer that for Si(111) $3 \times 1$ -Li,  $E_F - E_{\text{VBM}} = 0.43$  eV.

The deconvolution of the Si  $2p$  core-level spectrum of Si(111) $2 \times 1$  can be understood as follows.<sup>29</sup> The  $\pi$ -bonded Si chains of Si(111) $2 \times 1$  exhibit a Jahn-Teller instability which induces a buckling of the chains, accompanied by a charge transfer from the inward relaxed chain atoms to the outward relaxed chain atoms. Accordingly, the high-binding-energy core of Si(111) $2 \times 1$  has been attributed to the

TABLE I. Fitting parameters of the Si  $2p$  core-level spectrum of Si(111) $3 \times 1$ -Li (Fig. 7). The branching ratio of the  $2p_{3/2}$  and  $2p_{1/2}$  components was fixed at 0.5. The spin-orbit splitting is 0.606 eV. The Gaussian full width at half maximum (FWHM) is 0.43 eV.

Core level	$\Sigma_1$	$\Sigma_2$	Bulk
Kinetic energy Si $2p_{3/2}$ (eV)	14.86	15.72	15.26
Relative intensity $I/I_{\text{total}}$	0.138	0.138	0.724
Lorentzian FWHM (eV)	0.150	0.150	0.150

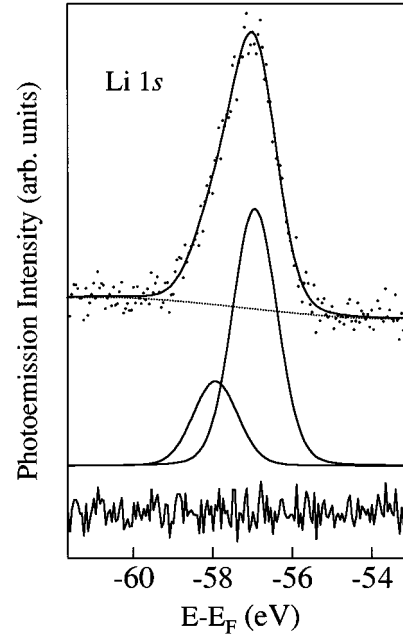


FIG. 8. Li  $1s$  core-level spectrum, fitted with two components. The background is a third-order polynomial function. Fitting parameters are given in Table II. The photon energy is 91.32 eV.

“down-atoms” of the buckled  $\pi$ -bonded Si chains; the low-binding-energy core has been attributed to the “up-atoms.”<sup>29</sup> A tentative conclusion would be that the  $\pi$ -bonded Si chains of the Si(111) $3 \times 1$ -Li reconstruction are also buckled, consistent with the LDA calculations. However, naively one would also expect a *chemically shifted* component for the Si atoms neighboring the alkali. This third component is absent but most likely coincides with the bulk core level. This is not unreasonable considering the fact that other alkali/Si interfaces also lack any appreciable chemical shift of the Si  $2p$  core level.<sup>31</sup> The alternative interpretation is that the high-binding-energy core is associated with the alkali-bonded Si atoms and that the low-binding-energy core corresponds to the  $\pi$ -bonded chains.<sup>18</sup> This, however, is highly unlikely because it would require an intensity ratio of 1:2. Based on the similarity between the core levels of Si(111) $2 \times 1$  and Si(111) $3 \times 1$ -Li we conclude that the Si  $2p$  core-level of Si(111) $3 \times 1$ -Li is consistent with a *buckling* of the  $\pi$ -bonded Si chain.

The Li  $1s$  core level is displayed in Fig. 8 (see also Table II). First of all, we note that the binding energy of the main line is exceptionally high (56.9 eV), even higher than that of the Li  $1s$  core in most Li halides ( $\approx 56$ –57 eV).<sup>32</sup> This could be due to the ionic configuration of the Li atom, as indicated by the LDA calculations, or to the lack of final-state screening at this nonmetallic interface, or perhaps both. Interest-

TABLE II. Fitting parameters of the Li  $1s$  core-level spectrum of Si(111) $3 \times 1$ -Li (Fig. 8). The Gaussian FWHM is 1.25 eV.

Core level	Main line	Satellite
Binding energy Li $1s$ (eV)	56.9	57.9
Relative intensity $I/I_{\text{total}}$	0.75	0.25
Lorentzian FWHM (eV)	0.125	0.125

ingly, the Li  $1s$  core cannot be fitted with a single component. As can be seen, there is a need to include a second component at higher binding energy. A similar observation has been made for Si(111) $3\times 1$ -Na.<sup>27,28</sup> According to Paggel *et al.*, the high binding-energy component corresponds to some alkali metal present at domain boundaries<sup>27</sup> or in some precursor state to the  $(3\times 1)$  structure.<sup>28</sup> However, the exceptionally high binding energy (57.9 eV) of this shoulder makes an interpretation in terms of a simple initial state picture questionable. It could perhaps represent a shake-up satellite. As pointed out previously, core-level spectra of alkali metals on various substrates tend to exhibit broad asymmetric line shapes and rather high binding energies, especially at very small coverage.<sup>33,34</sup>

### C. Buckling versus dimerization

Total-energy considerations slightly prefer the extended Pandey model over the Seiwatz reconstruction.<sup>20</sup> In addition, the calculated STM images of the extended Pandey model are in good agreement with experiment<sup>14,15</sup> whereas the agreement is poor for the *buckled* Seiwatz reconstruction.<sup>20</sup> However, the present study casts serious doubts on the extended Pandey model. The most salient feature of the extended Pandey model is the presence of a  $\pi$ -bonded surface state that has a large positive dispersion along the chains for wave vectors approaching the zone boundary.<sup>20</sup> This state is clearly absent in angle-resolved photoemission. The experimental data are consistent with the calculated dispersion for the buckled Seiwatz model along the main symmetry direction, i.e.,  $\bar{\Gamma}A$ . However, discrepancies exist at other  $k$  points in the  $3\times 1$  surface Brillouin zone.

We fully acknowledge the fact that the photoemission data from a three-domain surface should be interpreted with care. It is somewhat surprising that the experimental dispersion along the  $[1\bar{1}0]$  direction is much larger than along the  $[\bar{1}12]$ , exactly what one would expect for a single-domain surface. In addition, the dispersion along the  $[\bar{1}12]$  direction seems to follow the  $(3\times 1)$  periodicity. However, because we cannot deconvolute the contributions from the individual domains, the prominent surface state in Fig. 2(a) may be a superposition of unresolved states along the  $\bar{\Gamma}A$  and  $\bar{\Gamma}D$  directions. This does not prevent us from making some definite conclusions. In fact, the lack of an upward dispersing surface state along  $\bar{\Gamma}A$  is in *serious disagreement* with the extended Pandey model. The possibility that we may have missed this state because of symmetry selection rules<sup>25</sup> must be dismissed. The  $[1\bar{1}0]$  direction is not in a symmetry plane of the surface and hence, the  $\pi$ -bonded surface state does not have a definite parity with respect to the emission plane.

Given the discrepancy between the theoretical and experimental surface-state dispersion, we now consider possible resolutions. Broadly speaking, there are three distinct possibilities: (i) a completely different structural model; (ii) small structural distortions to either the Pandey or Seiwatz model with an accompanying change in the band structure; or (iii) electron correlation effects that alter the (quasiparticle) band structure but leave the atomic geometry unchanged. Although an entirely different model can never be ruled out, Erwin's LDA calculations have clearly identified the  $\pi$ -bonded chain models as the lowest total-energy

TABLE III. Consistencies (+) and inconsistencies (−) between the various experimental techniques, LDA calculations, and the proposed structural models. BP stands for buckled Pandey model. BS for buckled Seiwatz model, DP for dimerized Pandey model, and DS for the dimerized Seiwatz model. The symbol  $\circ$  means “unknown.” The angle-resolved photoelectron spectroscopy (ARPES) data are consistent with the buckled Seiwatz model from  $\bar{\Gamma}\rightarrow A\rightarrow K$  (see text).

Technique	BP	BS	DP	DS
STM	+	−	$\circ$	$\circ$
ARPES	−	+	$\circ$	$\circ$
Si $2p$ core level	+	+	−	−
DFT-LDA	+	+	−	−

configurations.<sup>20</sup> So far, no realistic alternatives have been put forth. We therefore discuss the latter two alternatives below.

A key structural unit of each of the two reconstruction models is a polysilenelike chain of Si atoms: in the Seiwatz model it essentially sits on the unreconstructed substrate, and in the Pandey model it forms the upper part of the sevenfold rings. The same chain occurs in the  $2\times 1$  Pandey reconstruction of Si(111),<sup>3</sup> and an analogous polyacetylenelike chain occurs in C(111) $2\times 1$ .<sup>35,36</sup> For the Si(111) $2\times 1$  and C(111) $2\times 1$  surfaces, the precise geometry and orientation of this chain have been the focus of much theoretical and experimental scrutiny. Two distinct displacive distortions are generally considered: tilting, or buckling, of the plane of the chain with respect to the surface plane; and dimerization along the chain. The former is often described as a band Jahn-Teller distortion, while the latter is a Peierls instability. For Si(111)- $2\times 1$ , precise LDA total-energy calculations show a substantial buckling ( $\sim 0.49$  Å), and no evidence for dimerization<sup>5</sup> whereas for the closely related C(111)- $2\times 1$  surface, identical calculations show substantial dimerization (1.4%) but no buckling.<sup>35,36</sup> The different behavior in Si and C is in part explained by carbon's larger Coulomb repulsion; since buckling is accompanied by charge transfer between the two inequivalent chain atoms, this distortion is costlier for C than for Si.<sup>35</sup> It is not clear, however, whether one distortion always preempts the other, as appears to be the case in Si(111) $2\times 1$  and C(111) $2\times 1$ .

For the Pandey model of Si(111) $3\times 1$ - $M$  ( $M=Li,Na,K,Rb$ ), Erwin's LDA total-energy calculations also found a buckled geometry without any evidence for dimerization,<sup>20</sup> consistent with the results for the Pandey reconstruction of Si(111)- $2\times 1$ ;<sup>5</sup> for the Si(111) $3\times 1$  Seiwatz model, the equilibrium geometry was also buckled and again no dimerization was found.<sup>37</sup> As a consequence of these buckled chain geometries, simulated STM images for the  $3\times 1$  Pandey model are consistent with experiment, while simulated images from the Seiwatz model were in strong contradiction. As we have noted, however, neither model leads to calculated dispersions in perfect agreement with experiment. Table III summarizes the above discrepancies.

In light of this discrepancy, we propose the possibility of *coexisting* static distortions, i.e., both buckling and dimerization. Three observations are pertinent. First, STM images from Si(111) $3\times 1$ -Li and Si(111) $3\times 1$ -Ag show a slight sym-

metry breaking that is qualitatively consistent with dimerization.<sup>15,38</sup> Second, the Si  $2p$  core levels are consistent with buckling. Third, detailed studies of hypothetical *trans*-polysilene (the analog of *trans*-polyacetylene) have shown that when electron correlation is included via many-body methods, substantial dimerization is predicted (8%); in contrast, density-functional theory with gradient corrections predicts only 1% dimerization.<sup>39</sup> Whether this result will carry over into the surface environment is at present not known, but it is clear that exchange and correlation should be treated at a more rigorous level than in the LDA. The consequences of a dimerization distortion for the surface-state dispersion are not clear, but we believe that substantial perturbations are plausible. At the very least, we speculate that including these effects may alter both the detailed geometrical and electronic structure of the proposed reconstruction models. In the case of the extended Pandey model, such coexisting distortions would have to reverse the dispersion of the  $\pi$ -bonded dangling-bond states, in order to obtain agreement with experiment. In the case of the Seiwatz model, however, additional dimerization should only significantly alter the dispersion along the upper edge of the Brillouin zone and leave the dispersion of the  $\pi$ -bonded dangling-bond state along  $[\bar{1}\bar{1}0]$  more or less intact. A similar scenario has been reported for  $C(111)2\times 1$  where the quasiparticle bands of the buckled and dimerized geometries have similar dispersion parallel to the  $\pi$ -bonded chains but opposite dispersion in other parts of the surface Brillouin zone.<sup>36</sup>

The second alternative we consider here is of purely electronic origin. Pankratov and Scheffler have recently discussed the importance of properly accounting for the Coulomb repulsion  $U$  in a Hubbard Hamiltonian to describe  $GaAs(110)-K$ .<sup>40</sup> This system shares several features with the metal-induced  $Si(111)3\times 1$  reconstruction: the alkali valence charge is almost completely transferred into surface dangling-bond states; several inequivalent dangling-bond sites are available in the unit cell; and the occupied surface states are narrow (less than 1 eV). For  $GaAs(110)-K$ ,  $U$  was found to be comparable to this bandwidth, indicating that the surface is in the Mott-Hubbard regime; including this term also introduced a zone-boundary energy gap of order  $U$ . While the situation for  $Si(111)3\times 1$  is more complex (there are three dangling bonds per cell and no zone-boundary degeneracy), the possibility of a correlated Hamiltonian leading to substantial changes in the detailed dispersion should be analyzed as well.

Finally, it is important to compare the present data with the photoemission study of a three-domain  $Si(111)3\times 1-K$  surface by Sakamoto *et al.*<sup>17</sup> and the LDA calculations for  $Si(111)3\times 1-Na$  by Jeong and Kang.<sup>21</sup> In their photoemission paper, Sakamoto *et al.* reported various surface states which could not be clearly resolved.<sup>17</sup> Nonetheless, these authors

claim to observe a surface state with *positive* dispersion parallel to the chains and interpreted this state as a  $\pi$ -bonded surface state. Based on the assumption that  $\pi$ -bonded chains should have a positive dispersion, they also arrived at the Seiwatz model; the issue of buckling versus dimerization was not discussed. However, in their photoemission data, this state was *only* visible as a very weak shoulder near  $30^\circ$  emission angle. We therefore believe that the study of Sakamoto *et al.* does not provide strong evidence for a  $\pi$ -bonded surface state with positive dispersion. In contrast, the present study of  $Si(111)3\times 1-Li$  reveals a *well-resolved* surface state that has a *negative* dispersion along  $[\bar{1}\bar{1}0]$ . LDA calculations by Jeong and Kang also predicted a negative dispersion for a simple  $\frac{1}{3}$  ML adatom reconstruction.<sup>21</sup> Even though their calculated dispersion seems to be in qualitative agreement with our experimental data, we dismiss this structure as a likely candidate because its total energy is well above that of the  $\pi$ -bonded chains models.<sup>20</sup>

#### IV. SUMMARY AND CONCLUSIONS

We presented angle-resolved photoemission data of the three-domain  $Si(111)3\times 1-Li$  reconstruction and compared the data with calculated dispersions for the Seiwatz model and extended Pandey model. Among the large variety of proposed structural models, these  $\pi$ -bonded chain models represent the lowest total-energy configuration. Nonetheless, the  $\pi$ -bonded chain surface state of the extended Pandey reconstruction could not be reproduced in experiment. The experimental dispersion along the main symmetry direction ( $\Gamma A$ ) seems qualitatively consistent with the theoretical predictions for the *buckled* Seiwatz model. However, serious discrepancies exist in other parts of the surface Brillouin zone. We believe that the LDA's failure to fully reproduce the experimental band dispersions indicates that electron correlations in  $\pi$ -bonded Si chains should be treated on a more rigorous basis than the LDA.

#### ACKNOWLEDGMENTS

We thank E. W. Plummer for fruitful discussions. Acknowledgement is made to the donors of The Petroleum Research Fund, administered by the American Chemical Society, for support of this research. Oak Ridge National Laboratory is managed by Lockheed Martin Energy Research Corporation for the United States Department of Energy under Contract No. DE-AC05-96OR22462. Computational work was supported by the Cornell Theory Center and by a grant of HPC time from the Department of Defense Shared Resource Center MAUI. Some computational results were obtained using the software program Plane Wave (Biosym Technologies).

<sup>1</sup>R. E. Schlier and H. E. Farnsworth, J. Chem. Phys. **30**, 917 (1959).

<sup>2</sup>K. Takayanagi, Y. Tanishiro, M. Takahashi, and S. Takahashi, J. Vac. Sci. Technol. A **3**, 1502 (1985); Surf. Sci. **164**, 367 (1985).

<sup>3</sup>K. C. Pandey, Phys. Rev. Lett. **47**, 1913 (1981); **49**, 223 (1982).

<sup>4</sup>F. J. Himpsel, P. M. Marcus, R. Tromp, I. P. Batra, M. R. Cook, F. Jona, and H. Liu, Phys. Rev. B **30**, 2257 (1984).

<sup>5</sup>F. Ancilotto, W. Andreoni, A. Selloni, R. Car, and M. Parrinello, Phys. Rev. Lett. **65**, 3148 (1990).

- <sup>6</sup>Y. G. Ding, C. T. Chan, and K. M. Ho, *Phys. Rev. Lett.* **67**, 1454 (1991).
- <sup>7</sup>L. S. O. Johansson, E. Landemark, C. J. Karlsson, and R. I. G. Uhrberg, *Phys. Rev. Lett.* **69**, 2451 (1992); Y. G. Ding, C. T. Chan, and K. M. Ho, *ibid.* **69**, 2452 (1992).
- <sup>8</sup>L. D. Marks and R. Plass, *Phys. Rev. Lett.* **75**, 2172 (1995).
- <sup>9</sup>T. Takahashi, S. Nakatani, N. Okamoto, T. Ishikawa, and S. Kikuta, *Jpn. J. Appl. Phys.* **27**, L 753 (1988).
- <sup>10</sup>E. Vlieg, A. W. Dernier van der Gon, J. F. van der Veen, J. E. McDonald, and C. Norris, *Surf. Sci.* **209**, 100 (1989).
- <sup>11</sup>E. J. van Loenen, J. E. Demuth, R. M. Tromp, and R. J. Hamers, *Phys. Rev. Lett.* **58**, 373 (1987); R. J. Wilson and S. Chiang, *ibid.* **58**, 369 (1987); **59**, 2329 (1987).
- <sup>12</sup>L. S. O. Johansson, E. Landemark, C. J. Karlsson, and R. I. G. Uhrberg, *Phys. Rev. Lett.* **63**, 2092 (1989).
- <sup>13</sup>M. Tikhov, L. Surnev, and M. Kiskinova, *Phys. Rev. B* **44**, 3222 (1991).
- <sup>14</sup>D. Jeon, T. Hashizume, T. Sakurai, and R. F. Willis, *Phys. Rev. Lett.* **69**, 1419 (1992).
- <sup>15</sup>K. J. Wan, X. F. Lin, and J. Nogami, *Phys. Rev. B* **46**, 13 635 (1992).
- <sup>16</sup>H. H. Weitering, N. J. DiNardo, R. Pérez-Sandoz, J. Chen, and E. J. Mele, *Phys. Rev. B* **49**, 16 837 (1994).
- <sup>17</sup>K. Sakamoto, T. Okuda, H. Nishimoto, H. Daimon, S. Suga, T. Kinoshita, and A. Kakizaki, *Phys. Rev. B* **50**, 1725 (1994).
- <sup>18</sup>T. Okuda, H. Shigeoka, H. Daimon, S. Suga, T. Kinoshita, and A. Kakizaki, *Surf. Sci.* **321**, 105 (1994).
- <sup>19</sup>H. Onishi, I. Katayama, Y. Ohba, and K. Oura, *Jpn. J. Appl. Phys.* **33**, 3683 (1994).
- <sup>20</sup>S. C. Erwin, *Phys. Rev. Lett.* **75**, 1973 (1995).
- <sup>21</sup>S. Jeong and M. Kang, *Phys. Rev. B* **51**, 17 635 (1995).
- <sup>22</sup>A. J. Heeger, S. Kivelson, J. R. Schrieffer, and W.-P. Su, *Rev. Mod. Phys.* **60**, 781 (1988).
- <sup>23</sup>G. C. L. Wong, C. A. Lucas, D. Loretto, A. P. Payne, and P. H. Fuoss, *Phys. Rev. Lett.* **73**, 991 (1994).
- <sup>24</sup>M. P. Teter, M. C. Payne, and D. C. Allan, *Phys. Rev. B* **40**, 12 255 (1989).
- <sup>25</sup>E. W. Plummer and W. Eberhardt, *Adv. Chem. Phys.* **49**, 533 (1982).
- <sup>26</sup>I. Ivanov, A. Mazur, and J. Pollmann, *Surf. Sci.* **92**, 365 (1980).
- <sup>27</sup>J. J. Paggel, H. Haak, W. Theis, and K. Horn, *J. Vac. Sci. Technol. B* **11**, 1439 (1993).
- <sup>28</sup>J. J. Paggel, G. Neuhold, H. Haak, and K. Horn, *Phys. Rev. B* **52**, 5813 (1995).
- <sup>29</sup>F. J. Himpsel, B. S. Meyerson, F. R. McFreely, J. F. Morar, A. Taleb-Ibrahimi, and J. A. Yarmoff, in *Photoemission and Absorption Spectroscopy of Solids and Interfaces*, Proceedings of the International School of Physics ‘‘Enrico Fermi’’ Course (CVII), edited by M. Campagna and L. Rosei (North-Holland, Amsterdam, 1989), p. 203.
- <sup>30</sup>F. J. Himpsel, G. Hollinger, and R. A. Pollack, *Phys. Rev. B* **28**, 7014 (1983).
- <sup>31</sup>P. Soukiassian, M. H. Bakshi, Z. Hurych, and T. M. Gentle, *Surf. Sci.* **221**, L 759 (1989); see also, P. Soukiassian and T. Kendelewicz, in *Metallization and Metal-Semiconductor Interfaces*, edited by I. P. Batra (Plenum, New York, 1989), p. 465, and references therein.
- <sup>32</sup>*Handbook of X-Ray Photoelectron Spectroscopy* (Perkin Elmer Corporation, Eden Prairie, MN, 1979).
- <sup>33</sup>H. H. Weitering, J. Chen, N. J. DiNardo, and E. W. Plummer, *Phys. Rev. B* **48**, 8119 (1993).
- <sup>34</sup>P. A. Brühwiler, G. M. Watson, and E. W. Plummer, *Surf. Sci.* **269-270**, 653 (1992).
- <sup>35</sup>S. Iarlari, G. Galli, F. Gygi, M. Parinello, and E. Tosatti, *Phys. Rev. Lett.* **69**, 2947 (1992).
- <sup>36</sup>C. Kress, M. Fiedler, and F. Bechstedt, *Europhys. Lett.* **28**, 433 (1994).
- <sup>37</sup>It is known that the LDA fails to reproduce the dimerization in *trans*-polyacetylene. It has been pointed out that a finite number of  $k$  points will lead to substantial problems in the mean-field Peierls picture of polyacetylene [see, e.g., J. W. Mintmire and C. T. White, *Phys. Rev. B* **35**, 4180 (1987); J. Ashkenazi, W. E. Pickett, H. Krakauer, C. S. Wang, B. M. Klein, and S. R. Chubb, *Phys. Rev. Lett.* **62**, 2016 (1989); J. Paloheimo and J. von Boehm, *Phys. Rev. B* **48**, 16 948 (1993)]. In our calculations, we sampled a dense logarithmic  $k$ -point mesh near the zone boundaries but we did not find evidence for a Peierls instability of the  $\pi$ -bonded Si chains. Alternatively, it has been argued that electron-electron correlation drives the dimerization in polyacetylene [G. Rossi, *Phys. Rev. B* **50**, 1268 (1994); G. König and G. Stollhoff, *Phys. Rev. Lett.* **65**, 1239 (1990)]. In that case, the LDA would not reproduce dimerization.
- <sup>38</sup>J. M. Carpinelli and H. H. Weitering, *Surf. Sci.* **331-333**, 1015 (1995); in this paper, STM images reveal the presence of zigzag chains, separated by linear chains. This is inconsistent with a pure buckling scenario: buckled zigzag chains appear as *linear* chains in STM [see, e.g., J. A. Stroscio, R. M. Feenstra, and A. P. Fein, *Phys. Rev. Lett.* **57**, 2579 (1986)].
- <sup>39</sup>S. Suhai, *Phys. Rev. B* **52**, 1674 (1995).
- <sup>40</sup>O. Pankratov and M. Scheffler, *Phys. Rev. Lett.* **70**, 351 (1993).